Crystallisation of fluoride-containing bioactive glasses

3 AUTHORS, INCLUDING:

Delia S Brauer
Friedrich Schiller University Jena
61 PUBLICATIONS **794** CITATIONS

SEE PROFILE

Robert G Hill
Queen Mary, University of London
272 PUBLICATIONS **4,046** CITATIONS

SEE PROFILE

Crystallisation of fluoride-containing bioactive glasses

Delia S. Brauer*, Robert G. Hill

Dental Physical Sciences, Institute of Dentistry, Barts and The London School of Medicine and Dentistry, Queen Mary University of London, Mile End Road, London E1 4NS, UK

Matthew D. O'Donnell

BSI UK, Davy Avenue, Milton Keynes MK5 8PP, UK

*Corresponding author. Tel.: +44 (0)207 882 5964; fax: +44 (0)207 882 7979. *E-mail address*: d.brauer@qmul.ac.uk.

Abstract

Fluoride prevents dental cavities, stimulates bone formation and inhibits bone resorption, and fluoride-containing bioactive glasses and glass-ceramics are of great interest for dental and orthopaedic applications. In a series of melt-derived bioactive glasses (SiO_2-P_2O_5-CaO-Na_2O-CaF_2) calcium fluoride was added in increasing amounts (0-32.7 mol% CaF_2) while keeping the network connectivity constant. Crystallisation temperatures were determined using differential scanning calorimetry. Glass powder was heat treated to crystallisation temperature at a heating rate of $10 \, K \, min^{-1}$ before cooling to room temperature. X-ray diffraction followed by Rietveld analysis showed crystal phases after heat treatment to be combeite, cuspidine and fluorite, with the relative amounts of combeite decreasing with increasing fluoride content in the glass while the relative amounts of the fluoride-containing phases increased. Formation of apatite during heat treatment could not be detected, owing to the low phosphate content (≤ 1.07 mol%) and too high a sodium content. As formation of apatite and particularly fluorapatite would be preferable for applications in dentistry and orthopaedics, future research will focus on higher phosphate content and low sodium content glasses.

Keywords

Biomaterials; Glasses; Crystallisation; Heat treatment; Rietveld analysis; Powder diffraction; Apatite; Fluorapatite; Combeite; Cuspidine; Fluorite

Introduction

Fluoride is well known to prevent dental cavities by inhibiting enamel and dentine demineralisation, enhancement of tooth remineralisation and inhibition of bacterial enzymes [1,2]. An important factor here is the formation of fluorapatite, which is more acid resistant than carbonated hydroxyapatite, the main component of enamel and dentine. Fluoride is also known to increase bone density, and despite a narrow therapeutic window and some dispute on effectiveness in prevention of fractures [3,4], fluoride-releasing implants might be of interest for patients suffering from osteoporosis.

Bioactive silicate glasses are of interest for use as bone grafts [5], implant coatings [6,7], in aluminium-free glass polyalkenoate (ionomer) bone cements [8] and even in dentifrices [9], and in all these applications addition of fluoride would be beneficial. Bioactive glass-ceramics based on combeite and wollastonite have been extensively studied [10], but their strength and bioactivity are less than ideal while FAp glass-ceramics have been shown to osseointegrate *in vivo* [11,12].

The aim of this study was to characterise glass structure and crystallisation behaviour of fluoride-containing bioactive glasses in order to develop bioactive glasses which crystallise to fluorapatite, rather than to phases such as combeite and wollastonite. Understanding the structure-property relationship in bioactive glasses and glass-ceramics enables us to design new compositions to give specific properties for applications as new generation biomaterials.

We characterised the crystallisation behaviour of melt-derived glasses SiO_2–P_2O_5–CaO–Na_2O with increasing concentrations of CaF_2. Network connectivity (NC, [13]) was fixed at 2.13 by adding CaF_2 while the ratio of all other components was kept constant.

Materials and methods

Glass synthesis

Glasses in the system SiO_2–P_2O_5–CaO–Na_2O were prepared using a melt–quench route. CaF_2 was added in increasing amounts (0 to 32.71 mol%) while network connectivity (NC) and the ratio of network former to network modifier were kept constant (glasses A to G, Table 1). In addition, a sodium-free version of glass C was synthesised (glass H, Table 1). Mixtures of analytical grade SiO_2 (Prince Minerals Ltd., Stoke-on-Trent, UK), P_2O_5, $CaCO_3$, Na_2CO_3 and CaF_2 (all Sigma-Aldrich, Gillingham, UK) were melted in a platinum-rhodium crucible for 1 h at 1430°C in an electric furnace (EHF 17/3, Lenton, Hope Valley, UK). A batch size of 100 g was used. After melting, the glasses were rapidly quenched into water

to prevent crystallisation. After drying, the glass was ground using a vibratory mill (Gyro mill, Glen Creston, London, UK) for 7 min and sieved using a 38 µm mesh analytical sieve (Endecotts Ltd., London, UK). All compositions were obtained in an amorphous state as confirmed by powder X-ray diffraction experiments (XRD; results not shown).

Table 1:   Synthetic glass composition in mol% and temperature of heat treatment (°C). Theoretical network connectivity is 2.13.

Glass	SiO_2	P_2O_5	CaO	Na_2O	CaF_2	T
A	49.47	1.07	23.08	26.38	0	695
B	47.12	1.02	21.98	25.13	4.75	582
C	44.88	0.97	20.94	23.93	9.28	660
D	42.73	0.92	19.94	22.79	13.62	587
E	40.68	0.88	18.98	21.69	17.76	650
F	36.83	0.80	17.18	19.64	25.54	612
G	33.29	0.72	15.53	17.75	32.71	478
H	44.88	0.97	44.87	0	9.28	745

Glass heat treatment and characterisation

Glass transition (T_g) and crystallisation temperatures were determined using differential scanning calorimetry (DSC, Stanton Redcroft DSC1500, Rheometric Scientific, Epsom, UK); 50 mg of glass were analysed in a platinum crucible using analytical grade alumina powder as reference with a heating rate of 10 K min^{-1}. Experiments were run using both glass frit and glass powder (< 38 µm). The processing window (PW) was calculated as the temperature difference between T_g and the onset of crystallisation ($T_{c,on}$).

For investigation of crystal phases, glass powder was heat-treated in an analogous fashion to DSC experiments: samples were heated in a porcelain furnace (Centurion Quartz, Dentsply Ceramco, York, PA, USA) to crystallisation peak ($T_{c,pk}$) temperature at a heating rate of 10 K min^{-1} before being allowed to cool to room temperature without holding at $T_{c,pk}$. Crystal phases were analysed using XRD (Phillips PW1700, 40 kV/40 mA, CuKα, data collected at room temperature).

For Rietveld analysis, Philips PC RD XRD files were converted to GSAS raw files using ConvX software. Rietveld analyses were performed using GSAS and EXPGUI software [14].

Results

Glass composition after melting was analysed previously [15], and showed fluoride losses up to 20%, but a linear relationship between nominal and analysed CaF_2 content.

DSC traces for both frit and glass powder are shown in Fig. 1. For all compositions, T_g was between 400 and 530°C. Apart from compositions A and B endotherms were below 900°C. Endotherms for glass D (both frit and powder) were upside down due to DSC set-up. All compositions apart from glass H clearly showed one or multiple exotherms (crystallisation peaks); only glass frit of composition H did not show any clear crystallisation peaks.
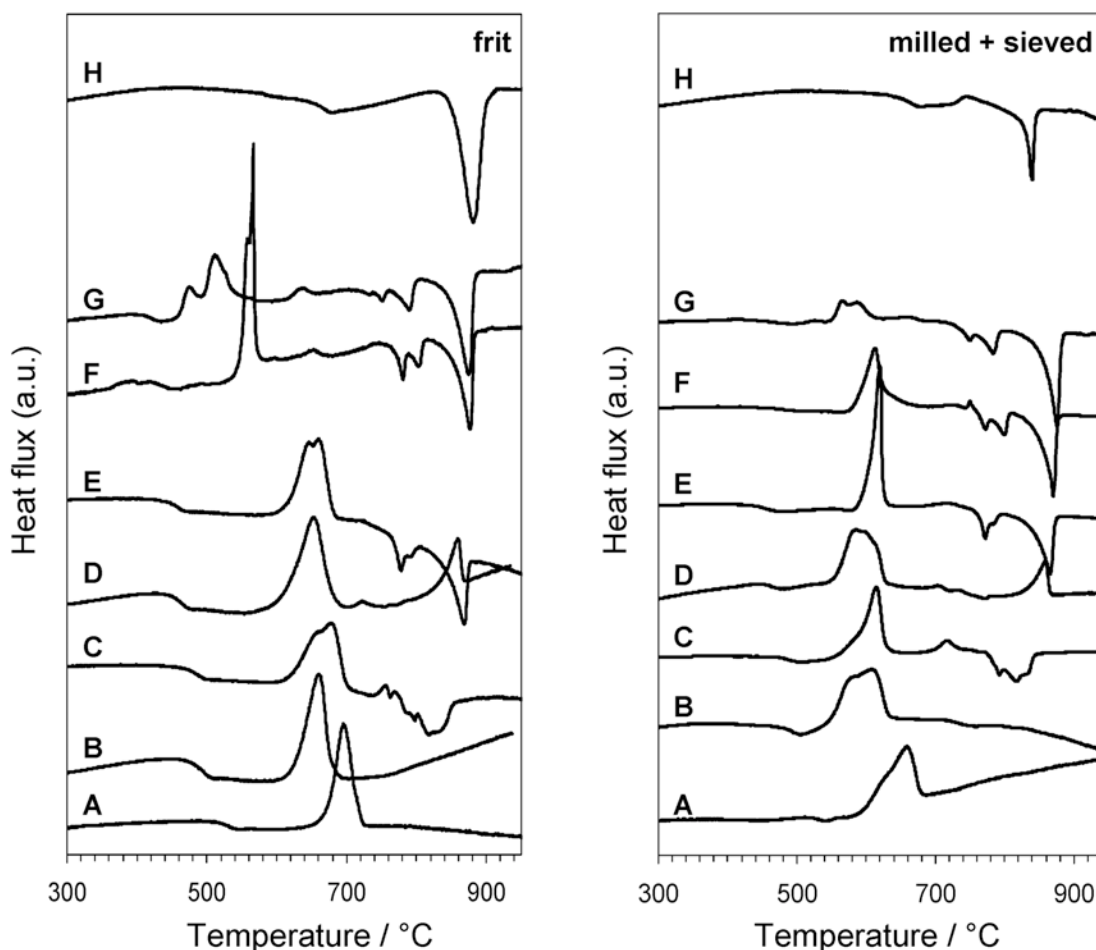

Figure 1:   DSC traces of glasses A to H for frit (left) and powder (right).

Glass transition (T_g), crystallisation onset ($T_{c,ons}$) and peak ($T_{c,pk}$) temperatures for frit and powder of glasses A to G showed a decrease in T_g with increasing CaF_2 content (Fig. 2). Crystallisation

Brauer et al., Phys. Chem. Glasses: Eur. J. Glass Sci. Technol. B 53(2) (2012) 27–30

6/13

temperatures of frit also decreased with CaF_2 content (Fig. 2a), but no such trend was observed for powder (Fig. 2b). Addition of CaF_2 up to 17.76 mol% (E) increased the processing window, while higher additions caused the PW to decrease (Fig. 3). T_g, $T_{c,ons}$ and $T_{c,pk}$ of glasses C and H (which is a sodium-free version of glass C) are compared in Table 2; Tg and crystallisation temperatures of glass H were significantly higher than those of glass C.

Table 2: Glass transition (T_g), crystallisation onset ($T_{c,on}$) and peak ($T_{c,pk}$) temperatures (°C) and processing window (K) of compositions C and H.

	glass	T_g	$T_{c,on}$	$T_{c,pk}$	PW
frit	C	466	618	662	152
	H	654	n/a	n/a	n/a
powder	C	475	586	615	111
	H	642	729	745	87

Crystal phases (Fig. 4a) after heat treatment were combeite ($Na_2Ca_2Si_3O_9$, glasses A to F), fluorite (CaF_2, glasses C to G) and cuspidine ($Ca_4Si_2O_7F_2$, glasses C to H). Both original data and fitted graph of heat-treated glass D are shown in Fig. 4b, while Fig. 5 shows the relative amounts of combeite, fluorite and cuspidine for glasses A to G. For glasses A to C, combeite was the main crystal phase. Apart from glass G (46 wt% fluorite), amounts of fluorite formed were small (less than 3 wt%). For sodium-free glass H, cuspidine was the only crystal phase formed. Combeite lattice parameters for glasses A to F (glasses G and H did not form combeite) showed changes with increasing CaF_2 content with the c-axis increasing in length with increasing CaF_2 content (Fig. 6).
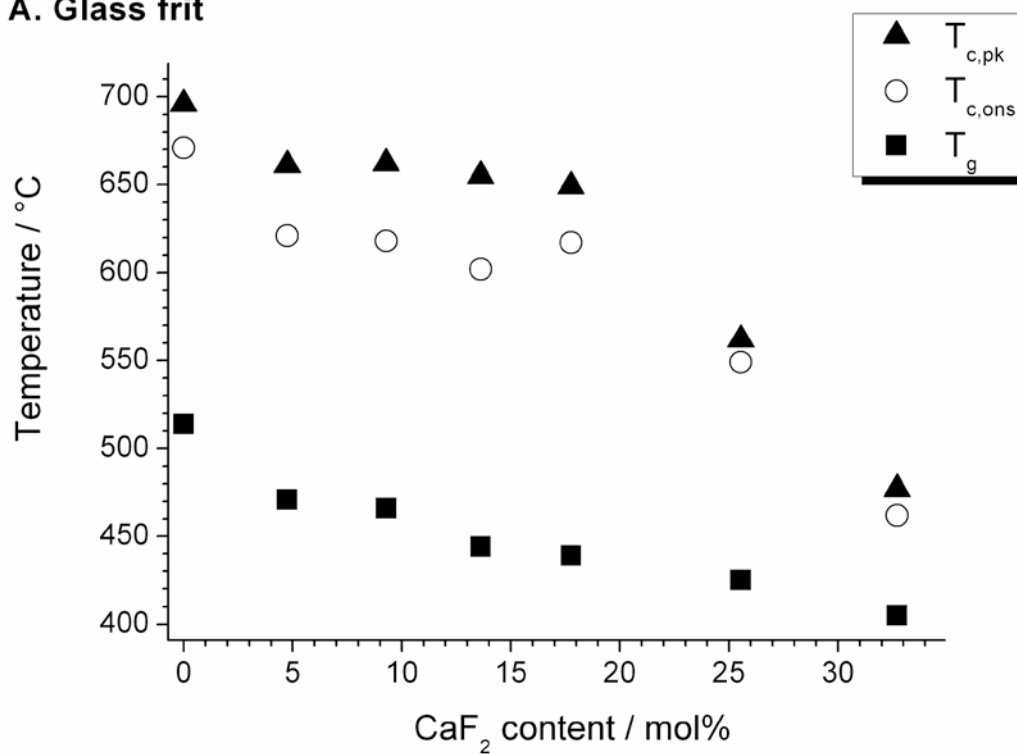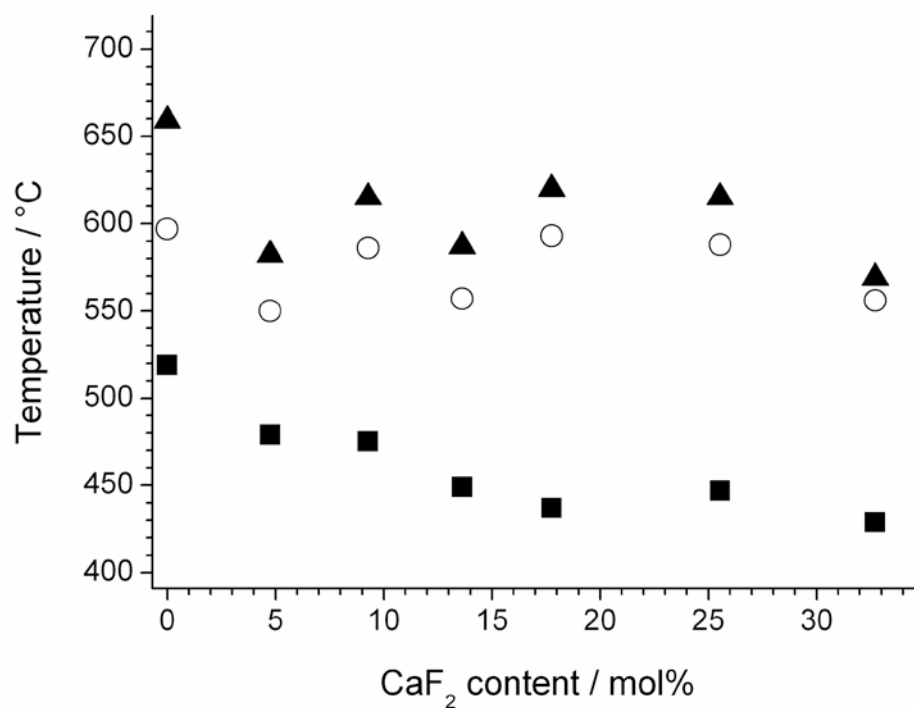
Figure 2: Glass transition temperature (T_g) as well as onset ($T_{c,on}$) and peak ($T_{c,pk}$) temperatures for the first crystallisation peak *vs*. CaF$_2$ content for (a) frit and (b) powder of glasses A to G.

Discussion

The glasses in this study have been previously shown to have a Q^2 silicate chain structure with a constant Q^3 content between 10 and 14% [16]. Glass transition and crystallisation temperatures decreased with increasing fluoride content, due to fluoride complexing calcium, resulting in CaF^+ structural units which provide less cross-linking than Ca^{2+} ions [17]. Addition of CaF_2 improved processing of the melt (by increasing the PW); only CaF_2 contents above 18 mol% resulted in a decreased PW. Glass H, which is a sodium-free version of glass C, showed a significantly higher T_g (642°C) than glass C (475°C). Again, this can be explained by differences in cross-linking of the silicate chains by network modifiers, due to Ca^{2+} being exchanged for Na^+ resulting in reduced electrostatic forces due to the smaller charge to size ratio of Na^+. For glasses A to E the crystallisation temperature decreased for decreasing particle size, indicating surface nucleation which is typical for combeite, the main crystal phase.
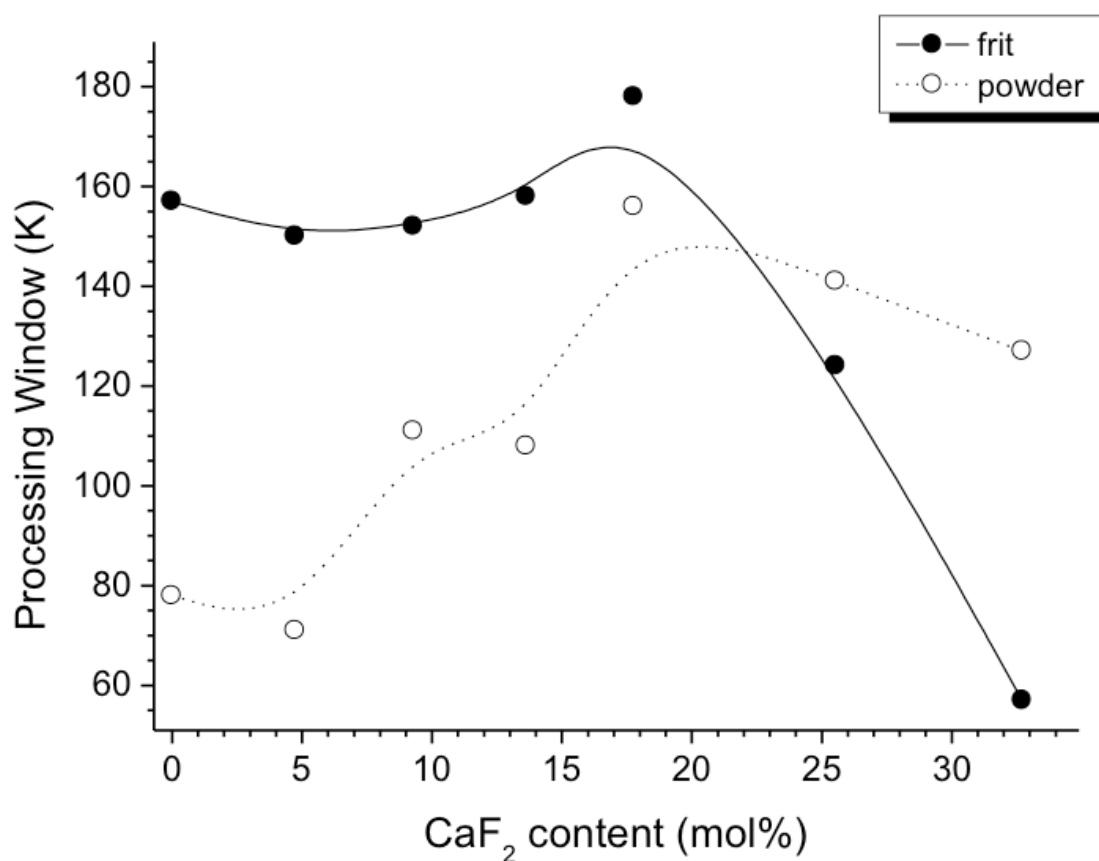

Figure 3: Processing window ($T_{c,on}$-T_g) *vs*. CaF_2 content.

As glasses A, B and H showed one crystal phase only upon heat treatment (Figs. 4a and 5), it was possible to assign exotherms and endotherms in DSC traces to crystal phases. The crystallisation peak (exotherm) and liquidus temperatures (endotherm; 880°C) for glasses A, B and H therefore correspond to cuspidine [18]. Glasses D to G also showed an endotherm at 880°C, which can be explained by either

melting of cuspidine or cuspidine dissolving into the glass phase. Although glasses A and B formed combeite only, their crystallisation temperatures differed. This difference in crystallisation temperature was caused by introduction of CaF_2, which reduced the viscosity of the glass melt and thus resulted in a lower crystallisation temperature for glass B compared to A.
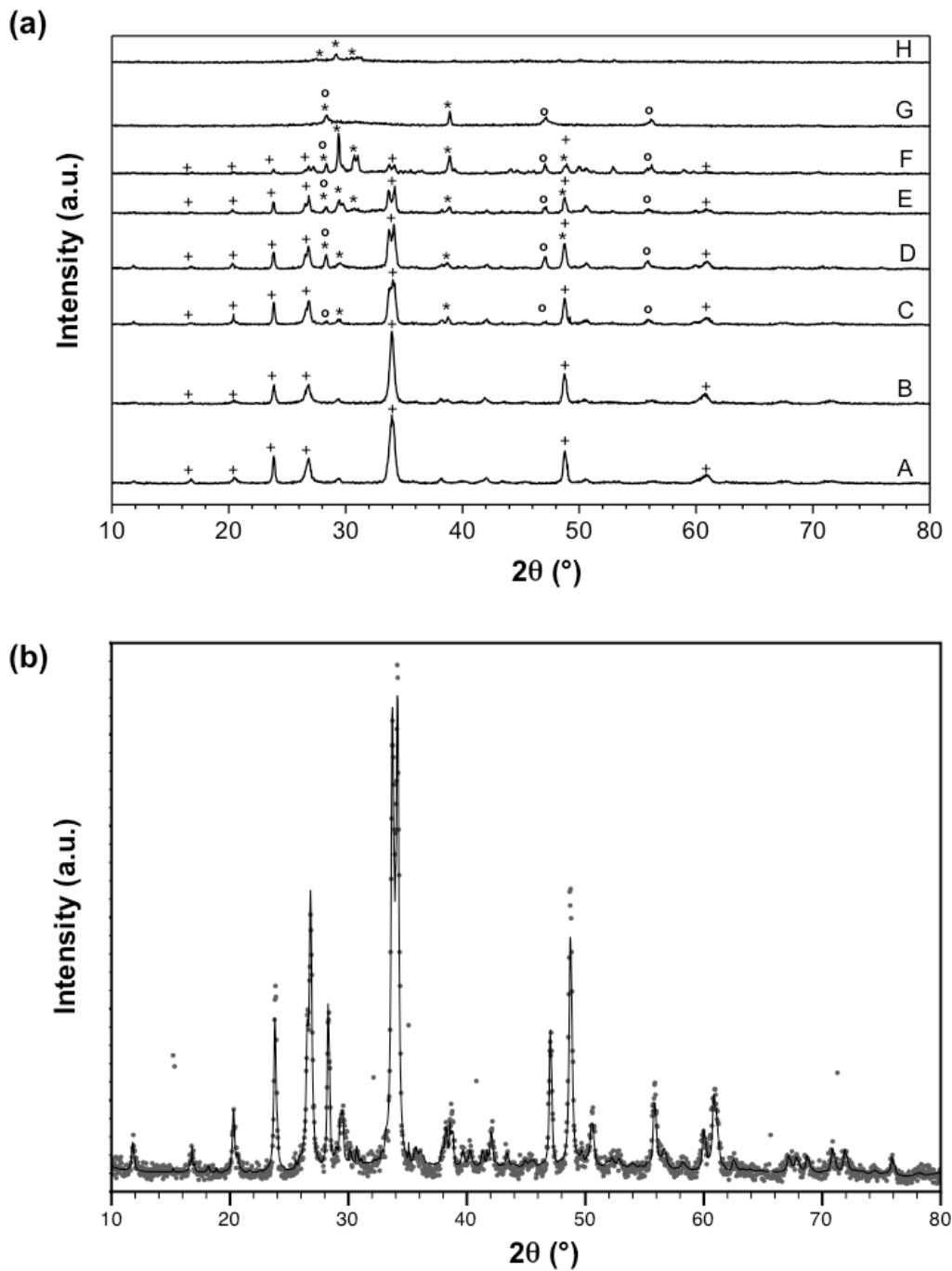

Figure 4: (a) XRD patterns of heat-treated crystalline samples A to H. Crystal phases are combeite (+), cuspidine (∗) and calcium fluoride (○). (b) Original XRD pattern (dots) and Rietveld fitting (line) of heat-treated glass D.

The exotherms for A and B shifted with particle size due to surface crystallisation, which is typical for combeite. Although only one crystal phase was formed, DSC traces for glass powder of compositions A and B showed double peaks, which could be explained by a combination of surface and bulk nucleation of combeite. Alternatively, it could be explained by solid solution of different phases: it was shown that mixed calcium sodium silicate glasses crystallise through the formation of solid solutions of several phases including combeite of different stoichiometry and a $Na_4CaSi_3O_9$ phase [10,19]. XRD data supports this theory: the main peak for combeite at about 34°2θ appeared as a single peak for glasses A and B while for glasses C to F it appeared as the typical split peak. It has been suggested previously that in sodium-rich glasses A and B additional precipitation of $Na_4CaSi_3O_9$ [19] gave the principal XRD peak at about 34°2θ overlapping with the split reflections of combeite.
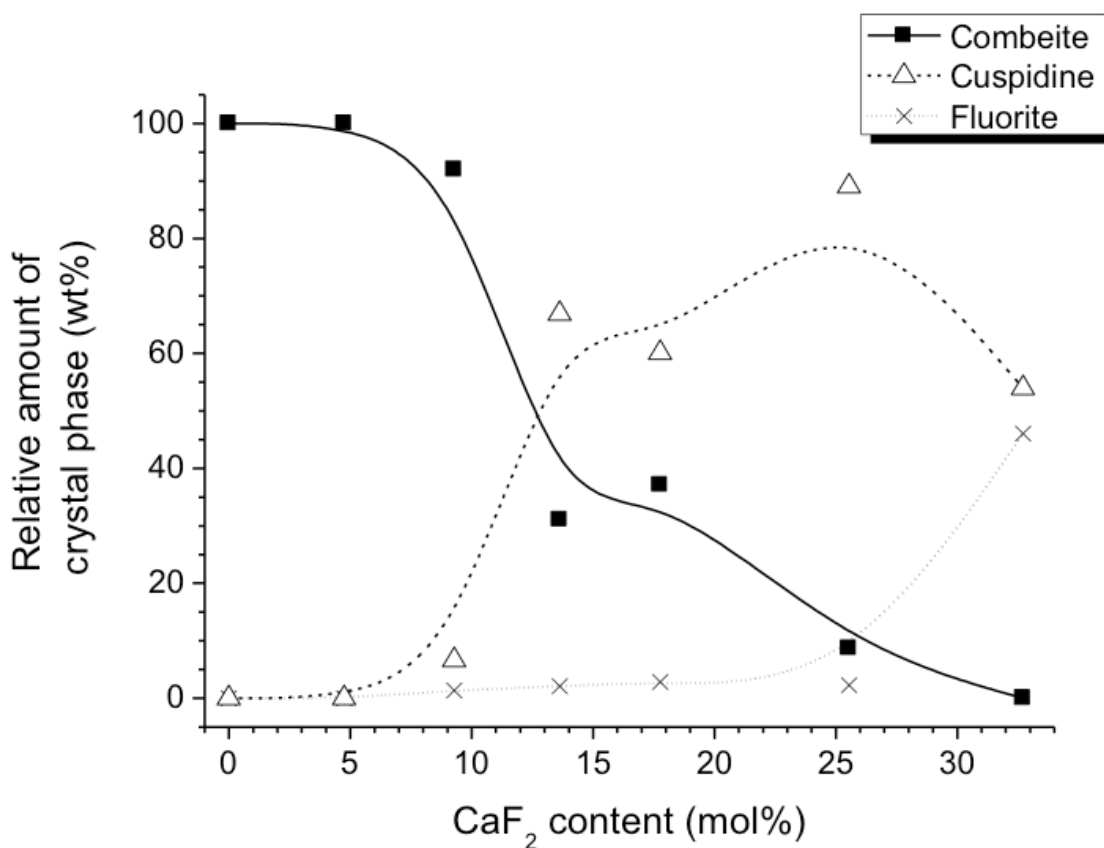

Figure 5:   Relative amount of crystal phases after heat treatment according to Rietveld analysis *vs*. CaF_2 content in the glass for glasses with increasing fluoride content (A to G).

With increasing CaF_2 content in the glass combeite was gradually replaced by the fluoride-containing phases cuspidine and fluorite, as shown by XRD results and Rietveld analysis. Simultaneously, the c-axis in combeite increased in length with increasing CaF_2 content, *i.e.* decreasing sodium content, in the glass,

which could be caused by vacancies in the lattice due to two Na^+ ions being replaced by Ca^{2+} or possibly by formation of a fluoridated combeite.
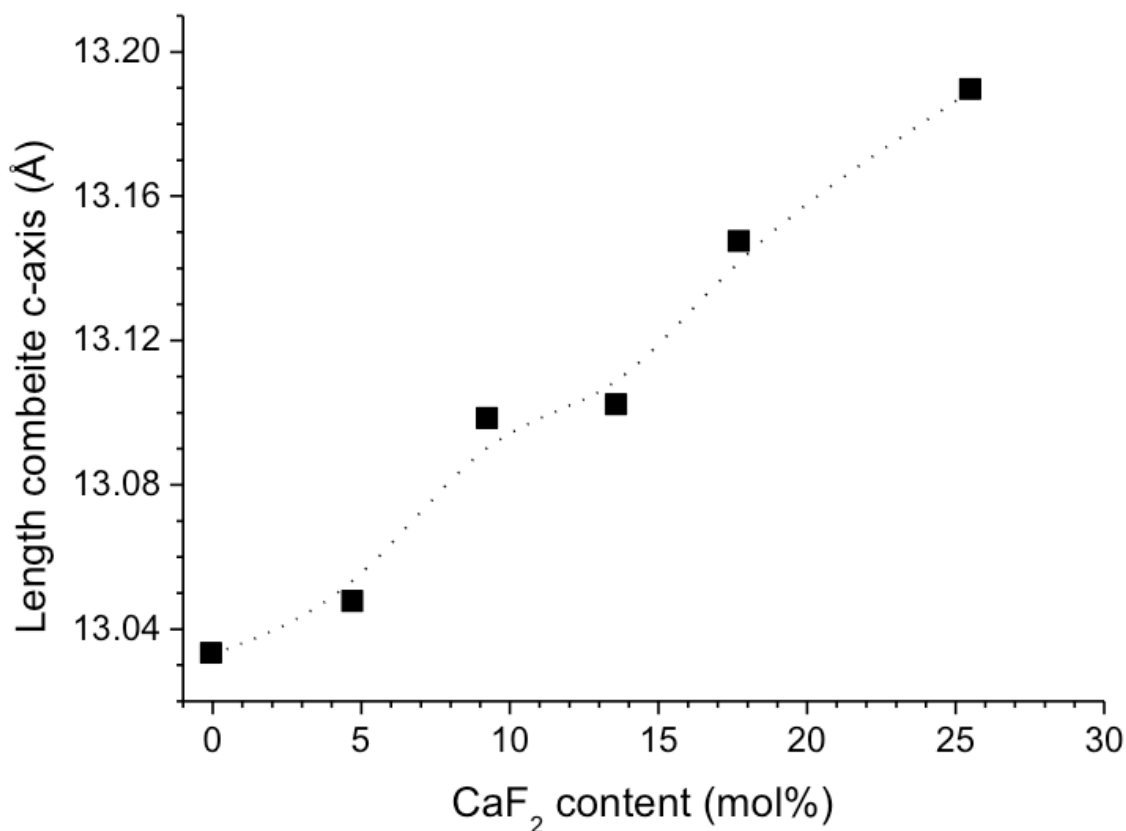

Figure 6:   Length of c-axis in combeite *vs*. CaF_2 content (glasses A to F).

Bioactive glasses are used in orthopaedic and dental applications, but also in dentifrices, and in all these glasses the release of fluoride would be beneficial. In addition, crystallisation of fluorapatite would be of great interest, particularly for dental applications due to its acid resistance. Lusvardi *et al*. investigated a similar glass system and reported formation of fluorapatite ($Ca_5(PO_4)_3F$) besides fluorite, cuspidine, nacaphite (Na_2CaPO_4F) and a $Na_2CaSi_2O_6$ phase when heat treating the glasses [20]. However, in the present glass system no fluorapatite was detected by either XRD or solid-state nuclear magnetic resonance spectroscopy [16]. This might be due to a very low phosphate content (≤ 1.07 mol% P_2O_5) compared to 2.6 mol% P_2O_5 in the Lusvardi study. Also, Lusvardi *et al*. found formation of FAp only in glasses with a low sodium content (19.3 mol% Na_2O or less), while the compositions in the present study (apart from G and H) contain more Na_2O. In bioactive glasses, phosphate is present as orthophosphate, PO_4^{3-}, charge balanced by sodium and calcium ions [16,21,22], and in high sodium content glasses the PO_4^{3-} tetrahedra are surrounded by too much Na^+ for apatite formation [20]. In order to design glasses

which crystallise to FAp, future research will focus on high phosphate content and low sodium content bioactive glasses.

Conclusions

Addition of small amounts of fluoride improved the processing of bioactive glasses. Upon heat treatment, fluoride-containing bioactive glasses crystallised to combeite, fluorite and cuspidine of varying relative amounts, depending on the calcium fluoride concentration in the glass. Fluorapatite, which would be of interest for dental and orthopaedic applications, did not form, but by increasing the phosphate concentration and decreasing the sodium oxide concentration in the glass crystallisation of fluorapatite could be favoured.

References

[1] Thuy, T. T., Nakagaki, H., Kato, K., Phan, A. H., Inukai, J., Tsuboi, S., Nakagaki, H., Hirose, M. N., Igarashi, S. & Robinson, C. Effect of strontium in combination with fluoride on enamel remineralization in vitro. *Archives of Oral Biology* 2008, **53**, 1017-1022. (doi:10.1016/j.archoralbio.2008.06.005)

[2] Featherstone, J. D. B. The science and practice of caries prevention. *Journal of the American Dental Association* 2000, **131**, 887-899.

[3] Aaseth, J., Shimshi, M., Gabrilove, J. L. & Birketvedt, G. S. Fluoride: A toxic or therapeutic agent in the treatment of osteoporosis? *Journal of Trace Elements in Experimental Medicine* 2004, **17**, 83-92.

[4] Vestergaard, P., Jorgensen, N. R., Schwarz, P. & Mosekilde, L. Effects of treatment with fluoride on bone mineral density and fracture risk - a meta-analysis. *Osteoporosis International* 2008, **19**, 257-268.

[5] Hench, L. L.& Wilson, J. Bioceramics. *MRS Bulletin* 1991, **16**, 62-74.

[6] Lotfibakhshaiesh, N., Brauer, D. S. & Hill, R. G. Bioactive glass engineered coatings for Ti6Al4V alloys: Influence of strontium substitution for calcium on sintering behaviour. *Journal of Non-Crystalline Solids* 2010, **356**, 2583-2590. (doi:10.1016/j.jnoncrysol.2010.05.017)

[7] Gomez-Vega, J. M., Saiz, E., Tomsia, A. P., Oku, T., Suganuma, K., Marshall, G. W. & Marshall, S. J. Novel bioactive functionally graded coatings on Ti6Al4V. *Advanced Materials* 2000, **12**, 894-898.

[8] Towler, M. R., Crowley, C. M., Murphy, D. & O'Callaghan, A. M. C. A preliminary study of an aluminum-free glass polyalkenoate cement. *Journal of Materials Science Letters* 2002, **21**, 1123-1126.

[9] Tai, B. J., Bian, Z., Jiang, H., Greenspan, D. C., Zhong, J., Clark, A. E. & Du, M. Q. Anti-gingivitis effect of a dentifrice containing bioactive glass (NovaMin®) particulate. *Journal of Clinical Periodontology* 2006, **33**, 86-91. (doi:10.1111/j.1600-051X.2005.00876.x)

[10] Fokin, V. M. & Zanotto, E. D. Continuous compositional changes of crystal and liquid during crystallization of a sodium calcium silicate glass. *Journal of Non-Crystalline Solids* 2007, **353**, 2459-2468.

[11] Goodridge, R. D., Wood, D. J., Ohtsuki, C. & Dalgarno, K. W. Biological evaluation of an apatite-mullite glass-ceramic produced via selective laser sintering. *Acta Biomaterialia* 2007, **3**, 221-231.

[12] Freeman, C. O., Brook, I. M., Johnson, A., Hill, R. G. & Hatton, P. V. Osseointegration of novel ionomeric glass-ceramics. *Journal of Dental Research* 2000, **79**, 1184.

[13] Hill, R. G. & Brauer, D. S. Predicting the bioactivity of glasses using the network connectivity or split network models. *Journal of Non-Crystalline Solids* 2011, **357**, 3884-3887.

[14] Toby, B. H. EXPGUI, a graphical user interface for GSAS. *Journal of Applied Crystallography* 2001, **34**, 210-213.

[15] Brauer, D. S., Mneimne, M. & Hill, R. G. Fluoride-containing bioactive glasses: Fluoride loss during melting and ion release in tris buffer solution. *Journal of Non-Crystalline Solids* 2011, **357**, 3328-3333. (doi:10.1016/j.jnoncrysol.2011.05.031)

[16] Brauer, D. S., Karpukhina, N., Law, R. V. & Hill, R. G. Structure of fluoride-containing bioactive glasses. *Journal of Materials Chemistry* 2009, **19**, 5629-5636. (doi:10.1039/b900956f)

[17] Bills, P. M. Viscosities in silicate slag systems. *Journal of the Iron and Steel Institute* 1963, **201**, 133-140.

[18] Hill, R. G., Da Costa, N. & Law, R. V. Characterization of a mould flux glass. *Journal of Non-Crystalline Solids* 2005, **351**, 69-74.

[19] Schneider, J., Mastelaro, V. R., Panepucci, H. & Zanotto, E. D. ^{29}Si MAS NMR studies of Q^n structural units in metasilicate glasses and their nucleating ability. *Journal of Non-Crystalline Solids* 2000, **273**, 8-18.

[20] Lusvardi, G., Malavasi, G., Cortada, M., Menabue, L., Menziani, M. C., Pedone, A. & Segre, U. Elucidation of the structural role of fluorine in potentially bioactive glasses by experimental and computational investigation. *Journal of Physical Chemistry B* 2008, **112**, 12730-12739. (doi:10.1021/jp803031z)

[21] Elgayar, I., Aliev, A. E., Boccaccini, A. R. & Hill, R. G. Structural analysis of bioactive glasses. *Journal of Non-Crystalline Solids* 2005, **351**, 173-183.

[22] Lockyer, M. W. G., Holland, D. & Dupree, R. NMR investigation of the structure of some bioactive and related glasses. *Journal of Non-Crystalline Solids* 1995, **188**, 207-219.